



HAL
open science

Charge susceptibility and conductances of a double quantum dot

V. Talbo, M. Lavagna, T. Q. Duong, Adeline Crépieux

► **To cite this version:**

V. Talbo, M. Lavagna, T. Q. Duong, Adeline Crépieux. Charge susceptibility and conductances of a double quantum dot. *AIP Advances*, 2018, 8 (10), pp.101333. 10.1063/1.5043108 . hal-01896080

HAL Id: hal-01896080

<https://hal.science/hal-01896080>

Submitted on 16 Oct 2018

HAL is a multi-disciplinary open access archive for the deposit and dissemination of scientific research documents, whether they are published or not. The documents may come from teaching and research institutions in France or abroad, or from public or private research centers.

L'archive ouverte pluridisciplinaire **HAL**, est destinée au dépôt et à la diffusion de documents scientifiques de niveau recherche, publiés ou non, émanant des établissements d'enseignement et de recherche français ou étrangers, des laboratoires publics ou privés.

Charge susceptibility and conductances of a double quantum dot

V. Talbo, M. Lavagna, T. Q. Duong, and A. Crépieux

Citation: *AIP Advances* **8**, 101333 (2018); doi: 10.1063/1.5043108

View online: <https://doi.org/10.1063/1.5043108>

View Table of Contents: <http://aip.scitation.org/toc/adv/8/10>

Published by the *American Institute of Physics*



Don't let your writing
keep you from getting
published!

AIP | Author Services

Learn more today!

Charge susceptibility and conductances of a double quantum dot

V. Talbo,¹ M. Lavagna,^{1,a} T. Q. Duong,² and A. Crépieux²

¹Univ. Grenoble Alpes, CEA, INAC, PHELIQS, F-38000 Grenoble, France

²Aix Marseille Univ, Université de Toulon, CNRS, CPT UMR 7332, 13288 Marseille, France

(Received 5 June 2018; accepted 2 October 2018; published online 12 October 2018)

We calculate the charge susceptibility and the linear and differential conductances of a double quantum dot coupled to two metallic reservoirs both at equilibrium and when the system is driven away from equilibrium. This work is motivated by recent progress in the realization of solid state spin qubits. The calculations are performed by using the Keldysh nonequilibrium Green function technique. In the noninteracting case, we give the analytical expression for the electrical current and deduce from there the linear conductance as a function of the gate voltages applied to the dots, leading to a characteristic charge stability diagram. We determine the charge susceptibility which also exhibits peaks as a function of gate voltages. We show how the study can be extended to the case of an interacting quantum dot. © 2018 Author(s). All article content, except where otherwise noted, is licensed under a Creative Commons Attribution (CC BY) license (<http://creativecommons.org/licenses/by/4.0/>). <https://doi.org/10.1063/1.5043108>

I. INTRODUCTION

The idea introduced two decades ago of a quantum computer based on solid state spin qubits¹ has led to an intensive effort in the realization of spin qubits on the basis of double quantum dots.²⁻⁴ The basic idea is to manipulate the spin encoded in the first of the quantum dots by means of various dc or ac external fields, then use the quantum exchange interdot coupling to carry out two-qubit operations, and finally readout the information on the spin encoded in the second quantum dot. The challenge becomes all the more accessible now that long spin coherence time has been recently achieved for individual spin qubits^{5,6} which ensures high-fidelity to quantum computation operations.⁷ This quest for realizing solid state quantum bits has motivated parallel theoretical studies on double quantum dots. The electron-electron interactions when present have been taken into account in a capacitive model with an additional interdot capacitance. It has thus been possible to establish the charge stability diagram of these systems in which the Coulomb oscillations of conductance observed in a single quantum dot are changed into a characteristic honeycomb structure as a function of the gate voltages applied to each dot.^{8,9} Another topic that has been widely discussed in the last years on both experimental and theoretical sides, is the possibility of exposing the double quantum dot to an electromagnetic radiation (i.e. to an ac external field) allowing the transfer of an electron from one to the other reservoir even at zero bias voltage.¹⁰⁻¹⁵ In this way, ac-driven double quantum dots act as either charge or spin pumps. The transport can then be either incoherent via sequential tunneling processes or coherent via inelastic cotunnelling processes. Most of the theoretical studies so far have been done by using the master equations^{12,15} or real time diagrammatic approach¹⁴ or time evolution of the density matrix.^{10,13} It is worth noting that even if these methods make it possible to describe the regimes of either weak or strong interdot tunnel coupling, their domain of validity is mainly restricted to the regime of weak tunneling between the dots and the reservoirs. We propose in this paper to develop a study of the double quantum dot in the framework of the Keldysh non-equilibrium Green function technique (NEGF) following the same strategy as we developed^{16,17}

^aElectronic mail: mireille.lavagna@cea.fr

before for a single quantum dot, i.e. by starting from the noninteracting case and then incorporating interactions by using the Keldysh NEGF technique. We present here the method and the results obtained in the case of a noninteracting double quantum dot. We give the analytical expression for the electrical current as a function of the Green functions and deduce from there the linear and differential conductances. In order to meet the concerns of experimentalists who have directly access to charge susceptibility via reflectometry measurements,¹⁸ we establish the charge susceptibility of a double quantum dot related to the mesoscopic capacity. This study brings the foundations for further studies to come on interacting double quantum dots where the geometric configuration offers the possibility of observing Pauli spin blockade in addition to the standard Coulomb charge blockade.

II. MODEL

We consider two single-orbital quantum dots 1 and 2 with spin degeneracy equal to 2 ($\sigma = \pm 1$) coupled together in series through a tunnel barrier with a hopping constant t_σ , and connected to two metallic reservoirs L and R through spin-conserving tunnel barriers with hopping constants $t_{L\sigma}$ and $t_{R\sigma}$ respectively. In the absence of interactions, the hamiltonian writes $H = H_{DQD} + H_{leads} + H_T$ with

$$\begin{aligned} H_{DQD} &= \sum_{\sigma} \left[\varepsilon_{1\sigma} d_{1\sigma}^{\dagger} d_{1\sigma} + \varepsilon_{2\sigma} d_{2\sigma}^{\dagger} d_{2\sigma} + t_{\sigma} d_{2\sigma}^{\dagger} d_{1\sigma} + t_{\sigma}^* d_{1\sigma}^{\dagger} d_{2\sigma} \right] \\ H_{leads} &= \sum_{k, \alpha \in (L, R), \sigma} \varepsilon_{k\alpha\sigma} c_{k\alpha\sigma}^{\dagger} c_{k\alpha\sigma} \\ H_T &= \sum_{k\sigma} \left[t_{L\sigma} c_{kL\sigma}^{\dagger} d_{1\sigma} + t_{L\sigma}^* d_{1\sigma}^{\dagger} c_{kL\sigma} + t_{R\sigma} c_{kR\sigma}^{\dagger} d_{2\sigma} + t_{R\sigma}^* d_{2\sigma}^{\dagger} c_{kR\sigma} \right] \end{aligned} \quad (1)$$

where $d_{i\sigma}^{\dagger}$ ($i=1$ or 2) is the creation operator of an electron with spin σ ($\sigma = \pm 1$) in the dot i with energy $\varepsilon_{i\sigma}$; $c_{k\alpha\sigma}^{\dagger}$ ($\alpha=L$ or R) is the creation operator of an electron with momentum k and spin σ in the lead α with energy $\varepsilon_{k\alpha\sigma}$. The energies $\varepsilon_{i\sigma}$ in the dots are tuned by the application of a dc gate voltage V_{Gi} on each dot. Since we are considering the noninteracting case in the absence of dot Coulomb interaction, all the results obtained in this paper are spin independent as though we were working with a spinless quantum dot system. For simplicity we will omit the σ subscript in the rest of the paper.

The retarded Green functions in the dots, $G_{1,1}^r(\omega)$, $G_{2,2}^r(\omega)$, $G_{1,2}^r(\omega)$ and $G_{2,1}^r(\omega)$, are solutions of the following Dyson equation written in matrix form along the $\{1, 2\}$ basis

$$\bar{G}^r(\omega) = \bar{G}^{(0)r}(\omega) + \bar{G}^{(0)r}(\omega) \bar{\Sigma}^r(\omega) \bar{G}^r(\omega) \quad (2)$$

where $\bar{G}^r(\omega)$ and $\bar{G}^{(0)r}(\omega)$ are respectively the exact and the unrenormalized Green functions in the dots, and $\bar{\Sigma}^r(\omega)$, the self-energies, defined as

$$\begin{aligned} \bar{G}^r(\omega) &= \begin{pmatrix} G_{1,1}^r(\omega) & G_{1,2}^r(\omega) \\ G_{2,1}^r(\omega) & G_{2,2}^r(\omega) \end{pmatrix} \\ \bar{G}^{(0)r}(\omega) &= \begin{pmatrix} (\omega - \varepsilon_1)^{-1} & 0 \\ 0 & (\omega - \varepsilon_2)^{-1} \end{pmatrix} \\ \bar{\Sigma}^r(\omega) &= \begin{pmatrix} \Sigma_L^r(\omega) & t^* \\ t & \Sigma_R^r(\omega) \end{pmatrix} \end{aligned} \quad (3)$$

where $\Sigma_{\alpha}^r(\omega) = |t_{\alpha}|^2 \sum_k (\omega - \varepsilon_{k\alpha} + i\eta)^{-1}$ (η being an infinitesimal positive). In the wide band limit: $\Sigma_{\alpha}^r(\omega) = -i\Gamma_{\alpha}(\omega)$ where $\Gamma_{\alpha}(\omega) = \pi |t_{\alpha}|^2 \rho_{\alpha}^{(0)}(\omega)$ and $\rho_{\alpha}^{(0)}(\omega)$ is the unrenormalized density of states in the reservoir α .

By solving Eq.(3), one obtains the following expressions for the Green functions in the dots

$$\begin{aligned} G_{1,1}^r(\omega) &= \frac{\omega - \varepsilon_2 - \Sigma_R^r(\omega)}{\mathfrak{D}^r(\omega)} \\ G_{1,2}^r(\omega) &= \frac{t^*}{\mathfrak{D}^r(\omega)} \\ G_{2,1}^r(\omega) &= \frac{t}{\mathfrak{D}^r(\omega)} \\ G_{2,2}^r(\omega) &= \frac{\omega - \varepsilon_1 - \Sigma_L^r(\omega)}{\mathfrak{D}^r(\omega)} \end{aligned} \quad (4)$$

with $\mathfrak{D}^r(\omega) = (\omega - \varepsilon_1 - \Sigma_L^r(\omega))(\omega - \varepsilon_2 - \Sigma_R^r(\omega)) - |t|^2$.

III. GENERAL EXPRESSION FOR THE CURRENT

We derive the expression for the current through the double quantum dot by using the Keldysh nonequilibrium Green function technique.

The current I_L from the L reservoir to the central region can be calculated from the time evolution of the occupation number operator in the L reservoir

$$I_L = -e \left\langle \frac{d\hat{n}_L(t)}{dt} \right\rangle = -ie \langle [\hat{H}, \hat{n}_L] \rangle \quad (5)$$

where $\hat{n}_L(t) = \exp(i\hat{H}t)\hat{n}_L \exp(-i\hat{H}t)$ is the number of electrons in the L reservoir in the Heisenberg representation (with $\hat{n}_L = \sum_{k,\alpha \in (L)} c_{k\alpha}^\dagger c_{k\alpha}$). The current I_R from the R reservoir to the central region can be defined in an analogous way.

Defining the lesser Green functions mixing the electrons in the dot and in the reservoir according to $G_{k\alpha,i}^<(t,t') = i \langle d_i^\dagger(t') c_{k\alpha}(t) \rangle$ and $G_{i,k\alpha}^<(t,t') = i \langle c_{k\alpha}^\dagger(t') d_i(t) \rangle$, the currents write

$$I_L = e \sum_k \left[t_L G_{1,kL}^<(t,t) - t_L^* G_{kL,1}^<(t,t) \right] \quad (6)$$

and a similar expression for I_R . The lesser Green functions $G_{k\alpha,i}^<(t,t')$ and $G_{i,k\alpha}^<(t,t')$ are then evaluated by applying the analytic continuation rules provided by the Langreth theorem¹⁹ to the Dyson equations for the Green functions. It results in

$$I_L = i \frac{e}{\pi} \int_{-\infty}^{\infty} d\omega \Gamma_L(\omega) \left[G_{1,1}^<(\omega) + n_F^L(\omega) (G_{1,1}^r(\omega) - G_{1,1}^a(\omega)) \right] \quad (7)$$

where $n_F^\alpha(\omega) = \frac{1}{e^{\beta(\omega - \mu_\alpha)} + 1}$ is the Fermi-Dirac distribution function in the reservoir α with chemical potential μ_α .

When the system is in the steady state, one gets:

$$I_L = \frac{2e}{\pi} \int_{-\infty}^{\infty} d\omega \Gamma_L(\omega) G_{1,2}^r(\omega) \Gamma_R(\omega) G_{2,1}^a(\omega) \left[n_F^L(\omega) - n_F^R(\omega) \right] \quad (8)$$

and $I_L = -I_R$, where $G_{i,j}^a(\omega)$ are the four advanced Green functions in the dots.

IV. CHARGE SUSCEPTIBILITY

In order to calculate the charge susceptibility of the system, one needs to connect each quantum dot i through a capacitance C_{ac}^i to an ac voltage $V_{ac}(t)$ (see Ref. 15), bringing the additional following term to the hamiltonian \hat{H} : $H_{ac}(t) = \sum_{i=1,2} e\alpha_i \hat{n}_{di} V_{ac}(t)$ where $\hat{n}_i = d_i^\dagger d_i$, the number of electrons in the dot i , and α_i measures the charge on the capacitance C_{ac}^i .

The total charge \hat{Q}_{ac} on the capacitances is given by

$$\hat{Q}_{ac} = \sum_{i=1,2} [-e\alpha_i \hat{n}_{di} e V_{ac}(t)] + (C_1^{(0)} + C_2^{(0)}) V_{ac} \quad (9)$$

where $C_1^{(0)}$ and $C_2^{(0)}$ are the capacitances of the two quantum dots when they are isolated (i.e. for $t = t_L = t_R = 0$).

From Eq.(9) and by using the linear response theory, one can obtain the charge susceptibility $\chi(t - t')$

$$\chi_{\sigma}(t - t') = -i\theta(t' - t) \sum_{ij} \alpha_i \alpha_j \langle [\hat{n}_{i\sigma}(t'), \hat{n}_{j\sigma}(t)] \rangle \quad (10)$$

By taking its Fourier transform, one gets the dynamical charge susceptibility $\chi(\omega)$ and in particular the static charge susceptibility in the $\omega = 0$ limit. The static charge susceptibility can simply be derived from

$$\chi(\omega = 0) = \sum_{ij} \alpha_i \alpha_j \frac{\partial \langle \hat{n}_i \rangle_0}{\partial \varepsilon_j} \quad (11)$$

where $\langle \hat{n}_i \rangle_0$ is the expectation value of the occupancy in the dot i at $V_{ac}(t) = 0$, which can be calculated from the lesser Green functions by using: $\langle \hat{n}_i \rangle = -\frac{i}{2\pi} \int d\omega G_{i,i}^<(\omega)$. In the case when both $\Gamma_{\alpha}(\omega)$ is independent on ω , it is straightforward to calculate $\langle \hat{n}_i \rangle_0$ and then take its derivative with respects to ε_j which allows to find the charge susceptibility $\chi(\omega = 0)$.

V. RESULTS

The color-scale plots of the linear conductance are shown in FIG. 1 as a function of the energy levels ε_1 and ε_2 in the dots for $\mu_L = \mu_R = 0$ at four different temperatures. FIG. 2 reports the dependence of G with the energy ε_1 along the first diagonal $\varepsilon_1 = \varepsilon_2$ of the previous figure. The state of the system with occupation numbers n_1 and n_2 in each dot is denoted as (n_1, n_2) . At low temperature, the states $(0, 0)$ and $(2, 2)$ are clearly separated from the $(0, 2)$ and $(2, 0)$ states by two conductance peaks thanks to the effect of the finite interdot hopping term t . With increasing temperatures, this frontier is getting blurrier and the conductance is higher along the $(0, 2) - (2, 0)$ frontier.

FIG. 3 shows the static charge susceptibility $\chi(\omega)$ at $T = 1$ K and $\mu_L = \mu_R = 0$ for four different configurations of couplings to the reservoirs, capacitances α_L, α_R (related to the geometry of the

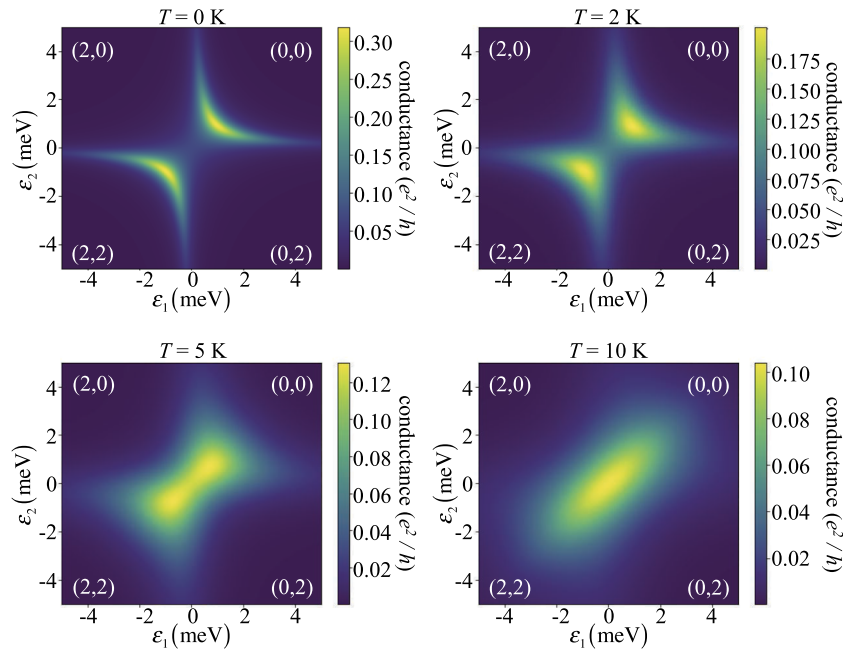


FIG. 1. Color-scale plots of the linear conductance G of the noninteracting double quantum dot as a function of the energy levels ε_1 and ε_2 in the dots for $\Gamma_L = \Gamma_R = 0.25$ meV (symmetric couplings), $t = 1$ meV and $\mu_L = \mu_R = 0$ at four different temperatures $T = 0, 2, 5, 10$ K. (n_1, n_2) denotes the state of the system with occupation numbers n_1 and n_2 in each dot.

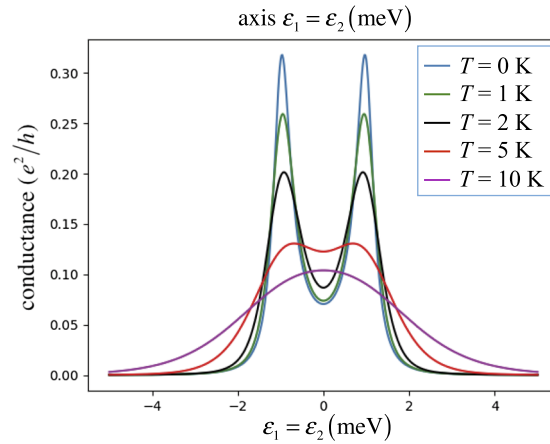


FIG. 2. Linear conductance G as a function of the energy ε_1 along the first diagonal $\varepsilon_1 = \varepsilon_2$ of the plots in FIG. 1 at five different temperatures $T = 0, 1, 2, 5, 10$ K.

device) and interdot hopping t . It shows the existence of peaks for the static charge susceptibility in the $(\varepsilon_1, \varepsilon_2)$ plane along two arcs located in the 1st and 3rd quadrants ($\varepsilon_1 > 0, \varepsilon_2 > 0$, and $\varepsilon_1 < 0, \varepsilon_2 < 0$ respectively). The corner spaces encircled by these two arcs correspond to the regimes (0,0) and (2,2) respectively. The central region between the two arcs corresponds to the other two regimes (0,2) and (2,0). As can be seen, the charge susceptibilities are equal in both (0,0) and (2,2) regimes, but differ from the one observed in the (0,2) and (2,0) regimes. This can be easily understood on the basis of the following physical argument. Let us first point out that in the limit $t \ll (\Gamma_L, \Gamma_R)$, the peaks in $\chi(\omega)$ occur near the two horizontal and vertical axes delimiting the four (0,0), (2,0), (2,2), (0,2) regimes, with an equal $\chi(\omega)$ in each quadrant brought by the intradot transition contributions

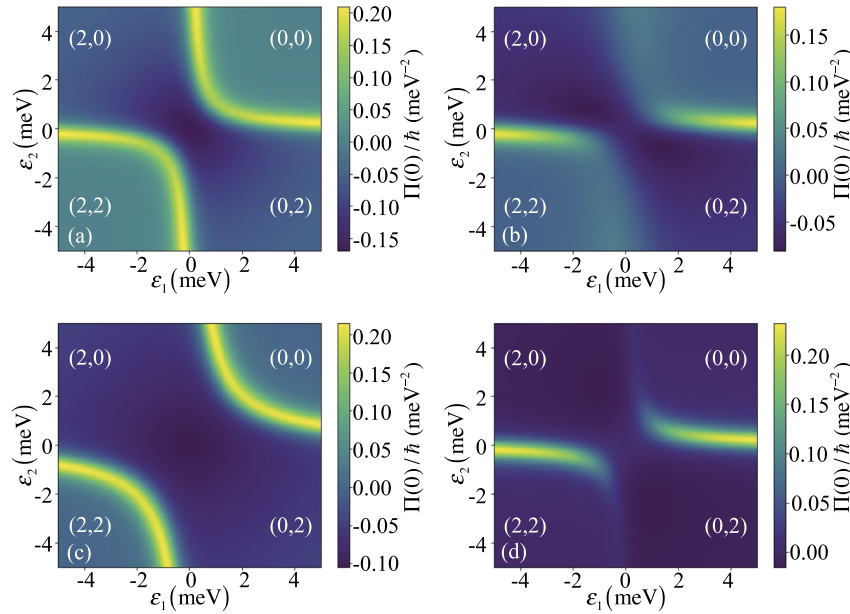


FIG. 3. Color-scale plots of the static charge susceptibility $\chi(0)$ of the noninteracting double quantum dot as a function of the energy levels $\varepsilon_{1\sigma}$ and $\varepsilon_{2\sigma}$ in the dots at $T = 1$ K and $\mu_L = \mu_R = 0$ for four sets of parameters (a) $\Gamma_{L\sigma} = \Gamma_{R\sigma} = 0.25$ meV (symmetric couplings), $\alpha_L = \alpha_R = -0.5$ (symmetric geometry), $t_\sigma = 1$ meV; (b) $\Gamma_{L\sigma} = 5\Gamma_{R\sigma} = 1.25$ meV (asymmetric couplings), $\alpha_L = \alpha_R = -0.5$ (symmetric geometry), $t_\sigma = 1$ meV; (c) $\Gamma_{L\sigma} = \Gamma_{R\sigma} = 0.25$ meV (symmetric couplings), $\alpha_L = \alpha_R = -0.5$ (symmetric geometry), $t_\sigma = 2$ meV; and (d) $\Gamma_{L\sigma} = \Gamma_{R\sigma} = 0.25$ meV (symmetric couplings), $\alpha_R = 5\alpha_L = -0.5$ (asymmetric geometry); $t_\sigma = 1$ meV.

only (i.e. by the $\frac{\partial \langle \hat{n}_i \rangle_0}{\partial \varepsilon_i}$ terms). In the presence of a finite t , the latter pattern transforms into two arcs located in the 1st and 3rd quadrants respectively as mentioned above. The larger t is, the larger the distance between the two arcs is, as can be seen by comparing FIG. 3 a and c. Gradually as the two arcs are formed from the initial pattern, the contributions to the charge susceptibility brought by the interdot transitions (i.e. $\frac{\partial \langle \hat{n}_i \rangle_0}{\partial \varepsilon_j}$ with $i \neq j$) become more and more important, showing a strong dependence inside the $(\varepsilon_1, \varepsilon_2)$ plane. Consequently, $\chi(\omega)$ in the (0,0) and (2,2) regimes belonging to the two quadrants inside which the arcs are formed, differ from $\chi(\omega)$ in the other (0,2) and (2,0) regimes, which explains the difference observed in FIG. 3. The last comment concerns the role of an asymmetry in either dot-lead couplings or geometry of the device. As can be seen, the effect of an asymmetry is to reduce the intensity of $\chi(\omega)$ along one of the arms of the arcs.

VI. CONCLUSION

We have studied the linear and differential conductances as well as the charge susceptibility of a noninteracting quantum dot by using the Keldysh nonequilibrium Green function technique. The obtained expressions are exact and allows one to study the variation of the conductances and charge susceptibility with temperature and any parameters of the double quantum dot model, energy levels $\varepsilon_1, \varepsilon_2$ of the dots, Γ_L, Γ_R and interdot hopping t . We have then discussed the evolution of the stability diagram of the system with the different parameters. This work opens the way for extension to the case of a double quantum dot in the presence of Coulomb interactions as is relevant for spin-qubit silicon-based devices.

ACKNOWLEDGMENTS

For financial support, the authors acknowledge the Programme Transversal Nanosciences of the CEA and the CEA Eurotalents Program.

- ¹ D. Loss and D. P. DiVincenzo, *Phys. Rev. A* **57**, 120 (1998).
- ² N. C. van der Vaart, S. F. Godijn, Y. V. Nazarov, C. J. P. M. Harmans, J. E. Mooij, L. W. Molenkamp, and C. T. Foxon, *Phys. Rev. Lett.* **74**, 4702 (1995).
- ³ T. Fujisawa, T. H. Oosterkamp, W. G. van der Wiel, B. W. Broer, R. Aguado, S. Tarucha, and L. P. Kouwenhoven, *Science* **282**, 932 (1998).
- ⁴ T. H. Oosterkamp, S. F. Godijn, M. J. Uilenreef, Y. V. Nazarov, N. C. van der Vaart, and L. P. Kouwenhoven, *Phys. Rev. Lett.* **80**, 4951 (1998).
- ⁵ J. T. Muhonen, J. P. Dehollain, A. Laucht, F. E. Hudson, R. Kalra, T. Sekiguchi, K. M. Itoh, D. N. Jamieson, J. C. McCallum, A. S. Dzurak, and A. Morello, *Nature Nanotechnology* **9**, 986 (2014).
- ⁶ R. Maurand, X. Jehl, D. Kotekar-Patil, A. Corna, H. Bohuslavskyi, R. Laviéville, L. Hutin, S. Barraud, M. Vinet, M. Sanquer, and S. De Franceschi, *Nature Communications* **7**, 13575 (2016).
- ⁷ M. Veldhorst, J. Hwang, C. Yang, A. Leenstra, B. de Ronde, J. Dehollain, J. Muhonen, F. Hudson, K. M. Itoh, A. Morello *et al.*, *Nature Nanotechnology* **9**, 981 (2014).
- ⁸ K. A. Matveev, L. I. Glazman, and H. U. Baranger, *Phys. Rev. B* **54**, 5637 (1996).
- ⁹ W. G. van der Wiel, S. De Franceschi, J. M. Elzerman, T. Fujisawa, S. Tarucha, and L. P. Kouwenhoven, *Rev. Mod. Phys.* **75**, 1 (2002).
- ¹⁰ B. L. Hazelzet, M. R. Wegewijs, T. H. Stoof, and Y. V. Nazarov, *Phys. Rev. B* **63**, 165313 (2001).
- ¹¹ R. López, R. Aguado, and G. Platero, *Phys. Rev. Lett.* **89**, 136802 (2002).
- ¹² V. N. Golovach and D. Loss, *Phys. Rev. B* **69**, 245327 (2004).
- ¹³ R. Sánchez, E. Cota, R. Aguado, and G. Platero, *Phys. Rev. B* **74**, 035326 (2006).
- ¹⁴ R.-P. Riwar and J. Splettstoesser, *Phys. Rev. B* **82**, 205308 (2010).
- ¹⁵ A. Cottet, C. Mora, and T. Kontos, *Phys. Rev. B* **83**, 121311 (2011).
- ¹⁶ R. Zamoum, M. Lavagna, and A. Crépieux, *Phys. Rev. B* **93**, 235449 (2016).
- ¹⁷ A. Crépieux, S. Sahoo, T. Q. Duong, R. Zamoum, and M. Lavagna, *Phys. Rev. Lett.* **120**, 107702 (2018).
- ¹⁸ A. Crippa, R. Maurand, D. Kotekar-Patil, A. Corna, H. Bohuslavskyi, A. O. Orlov, P. Fay, R. Laviéville, S. Barraud, M. Vinet, M. Sanquer, S. De Franceschi, and X. Jehl, *Nano Letters* **17**, 1001 (2017).
- ¹⁹ H. Haug and A.-P. Jauho, *Quantum Kinetics in Transport and Optics of Semiconductors* (Springer Netherlands, 2008).